



An atomic scale Monte Carlo study of exchange bias in homogeneous/inhomogeneous core/shell $\text{Fe}_3\text{O}_4/\text{CoO}$ nanoparticles

Z. Nehme  · Y. Labaye · N. Yaacoub · J. M. Grenèche

Received: 25 April 2019 / Accepted: 4 September 2019 / Published online: 8 October 2019
© Springer Nature B.V. 2019

Abstract The present work focuses on the study of exchange-biased magnetic core/shell nanoparticles at the atomic scale. The nanoparticles (NPs) consist of a perfectly epitaxial crystalline cobalt oxide (CoO) shell on a magnetite (Fe_3O_4) core. The numerical core/shell is built by taken into account the spinel structure of the core (Fe_3O_4) and the face-centered cubic structure of the shell (CoO). Two different configurations of core/shell NPs were examined: homogeneous and inhomogeneous core/shell. Our magnetic simulations are based on a 3D classical Heisenberg model. Monte Carlo simulations performing single spin rotation are used to investigate the effect of exchange bias on the spin configurations and hysteresis loops of core/shell nanoparticles. The numerical results reveal, as expected, a significant hysteresis loop shift obtained for a weak interface coupling. In addition, the magnetization reversal is not perfectly uniform in space when the interfacial coupling is different from zero. Finally, the increase in the magnetic interfacial coupling produces an increase in coercive field and a decrease in the exchange bias field.

Keywords Magnetic nanoparticles · Core/shell structure · Modeling of nanoparticles · Monte Carlo simulation · Hysteresis loop · Exchange bias coupling · Interface effects

Introduction

Over the past three decades, magnetic nanoparticles (NPs) have acquired a large number of experimental, theoretical, and numerical interests. Indeed, these interests are due to the original physical properties of NPs which differ significantly from those of the bulk materials because they are strongly influenced by the confinement effect (Gleiter 1989). They have found broad and promising applications in various fields (Bader 2006) such as magnetic fluids (Duan et al. 2013), biomedicine (Tartaj et al. 2003) (e.g., contrast agent for magnetic resonance imaging (MRI) (Jun et al. 2008), therapeutic hyperthermia (Thorat et al. 2013), magnetic information storage devices (Terris and Thomson 2005), and permanent magnets (Balamurugan et al. 2012).

In the field of magnetic recording, the current challenge is to increase the storage density. In this context, particular attention was paid to the magnetic NPs due to their small size. The most important condition is that NPs retain their stable magnetization with time and temperature. However, below a critical size, as a result of size reduction, the magnetic stability of the materials decreases at a given temperature called the blocking temperature (T_B). Consequently, NPs present a superparamagnetic state preventing a difficult contribution in the field of magnetic recording (Bedanta and Kleemann 2009). This behavior can be overcome by exchange bias coupling (EB) (Skumryev et al. 2003). Indeed, EB results from the coupling between the spins at the interface common to the ferromagnetic (F) or ferrimagnetic (Fi) and the antiferromagnetic (AF)

Z. Nehme (✉) · Y. Labaye (✉) · N. Yaacoub · J. M. Grenèche
Institut des Molécules et Matériaux du Mans (IMMM), UMR CNRS 6283, Le Mans Université, 72085 Le Mans, France
e-mail: zeinabnehme.89@gmail.com
e-mail: Yvan.Labaye@univ-lemans.fr

phases, during cooling by the Néel temperature of the AF component. This interfacial phenomenon induces additional anisotropy which can increase T_B in the case of magnetic NPs, improving their performance in the ultra-high-density information storage area (Nogués et al. 2005). However, the study of EB in systems of NPs resulting from different magnetic phases (core/shell, shell/shell NPs) remains so complicated. Indeed, different parameters are involved such as surface and interface effects (absence of microstructure at the interface or value of surface anisotropy), inhomogeneity of NPs, presence of collective response (dipolar interactions, interparticle interactions), state of the interface (roughness), and thickness of the shell (Iglesias et al. 2008, O'Grady et al. 2010, Manna and Yusuf 2014, Binns et al. 2010). The study of the physics underlying the EB phenomenology, particularly in core/shell NPs, remains a subject of interest and controversy. For example, it has been reported that both surface and interface moments play an important role in the EB effect in the case of Fe/ γ -Fe₂O₃ core/shell NPs (Chandra et al. 2012), which is dominated by frozen spins at the interface between the core and the shell in the case of Fe/Fe₃O₄ core/shell NPs (Ong et al. 2012).

In this context, simulation techniques based on Monte Carlo (MC) methods can play an important role in giving a detailed microscopic description of the spin structure. It allows us to compare experimental results with the suggested model. To the best of our knowledge, a detailed modeling of magnetic core/shell nanoparticles taking into account all their characteristic properties (morphology, crystallographic structure) is still not solved. The proposed numerical models are therefore in continuous development in order to reproduce as closely as possible the observed experimental properties of the real system. For example, Zaim et al. conducted MC studies to investigate the influence of shell coupling, interface coupling, and crystal field on the critical and compensation temperatures by implementing Ising model on ferrimagnetic core/shell with different shapes as nanocubes (Zaim et al. 2009) or a single spherical particle (Zaim and Kerouad 2010). A more realistic model with Heisenberg spins was developed by (Zianni and Trohidou 1999) where they highlighted the role of surface anisotropy on the reversal mechanism of small AF NPs by associating uniaxial anisotropies to the particle core and a radial anisotropy for surface sites. In 2012, they proposed a mesoscopic model to simulate the properties of an assembly of core/shell NPs in Co/

CoO system (Margaris et al. 2012). Recent studies in this group show the existence of a robust EB in an inverted core/shell NPs (Estrader et al. 2013). According to (De et al. 2016), the division of the shell in different regions with random anisotropies is proposed to investigate the presence of crystallite in the experimental shell. However, in the models suggested above, the actual crystallographic structure of the phases constituting the core and the shell was not taken into account. The magnetic nature of these materials (ferromagnetic, antiferromagnetic) is considered but with a simplified cubic structure.

This work is devoted to the numerical study by means of MC simulations of core/shell magnetic NPs. The studied system is a stoichiometric magnetite core with a spinel structure coated by a face-centered shell of cobalt oxide (CoO). The particularity of such a system is its ability to have an epitaxial growth between the core (ferrimagnetic) and the shell (antiferromagnetic), so the interface effects such as EB could be enhanced (Gaudisson et al. 2014). To better understand the properties of our system, a detailed microscopic description becomes necessary. Therefore, the MC method seems to be the most appropriate to elucidate the intimate spin structure of the interface between the core and the shell. The particularity of our simulations is that we consider the crystallographic structure of the core and the shell, so the measured EB properties result from the contribution of the interface of a more realistic structure of magnetite and cobalt oxide. For this purpose, the paper is organized as follows: in “[Model and simulation](#),” we describe the model and the simulation details considered in our work. “[Results and discussion](#)” reports the results and discussions. Finally, “[Conclusion](#)” is devoted to our conclusions.

Model and simulation

Structural model

Our numerical sample consists of a Fe₃O₄ magnetite core surrounded by a cobalt oxide CoO shell. Magnetite and cobalt oxide belong to two different crystalline structures: spinel structure for magnetite and face-centered cubic for cobalt oxide with unit cell parameters 8.397 Å and 4.26 Å, respectively (Coey 2010). The difference in unit cell parameters allows the epitaxial growth of a cobalt oxide phase on a magnetite phase

($8.397 \approx 2 \times 4.26 \text{ \AA}$). Therefore, we used a three-step construction for the core/shell NP model (Fig. 1).

The steps in the construction of a core-shell NP are as follows:

a) Construction of the ferrite core:

We considered the inverse spinel structure with space group $Fd\bar{3}m$ of unit cell $\approx 8.4 \text{ \AA}$ and built a spherical magnetite particle of radius 25.2 \AA .

b) Construction of the shell:

To model the cobalt oxide shell, we considered atomic positions of a face-centered cubic cell with a 4.2 \AA unit cell. Thus, the shell is built by creating a hollow sphere of cobalt oxide of external radius 33.7 \AA , and internal radius 25.2 \AA . This internal radius has been chosen in order to be compatible with the size of the magnetite core.

c) Construction of the core/shell:

In the last stage of the construction, we assemble the magnetic core with the cobalt oxide shell. This assembly avoids any overlap between the atoms at the core/shell interface. This interface is defined by the spins in the outer layer of the core and the surrounding AF inner layer of the shell. Thus, we obtain a core/shell Fe_3O_4/CoO NP of 33.7 \AA radius, consisting of 7209 magnetic atoms. Indeed, the size of this NP was chosen to be smaller than the reference experimental NPs (10 nm) in order to minimize the calculation time. For example, a simulated annealing under same calculation conditions for a structure whose size is 1.5 greater than that of a small NP, the calculation time will be multiplied by 3.

Usually, core/shell nanoparticles are modeled by means of simple cubic structures consisting of ferromagnetic (Iglesias et al. 2007a; Kechrakos and Trohidou 1998) or ferrimagnetic (Zaim et al. 2009) core and antiferromagnetic shell or an AF core surrounded by a F shell (Vasilakaki et al. 2015). In this work, we considered the experimental structure of magnetite and cobalt oxide, which makes our sample much more complex than those discussed in the literature, but also much closer to the systems studied experimentally (Gaudisson et al. 2014). The atomic model presented here is an approximation of real NPs core/shell that remains essential to study the exchange bias in more detail. Indeed,

the atomic scale modeling of magnetic NPs allows a natural treatment of the effects of symmetry breaking, lack of coordination, interface morphology, frustration effects ... We note that our numerical work has been applied to a single nanoparticle for two reasons. The first one is due to the fact that in the frame of an atomic scale MC simulation, each spin is assimilated to a 3D vector, so when an assembly of NPs of that size is simulated, the number of spins becomes enormous and the calculations become time-consuming. The second one is the possibility of avoiding collective effects, generally present in experimental system in order to evaluate the internal properties.

Magnetic model

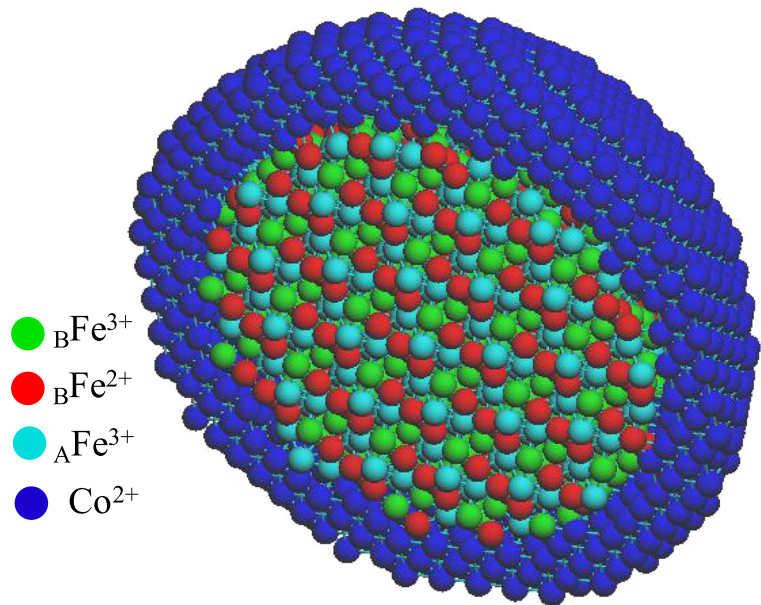
We compute the magnetic properties of the system by mean of a classical atomistic spin model with a three-dimensional Heisenberg Hamiltonian that reads as follows:

$$H = \sum_{i=0}^{N-1} \left[-\frac{1}{2} \sum_{j \in V} J_{ij} \vec{S}_i \cdot \vec{S}_j - C_H \vec{S}_i \cdot \vec{B}_{\text{ext}} + K_{Ui} \left(1 - \left(\vec{U}_i \cdot \frac{\vec{S}_i}{S_i} \right)^2 \right) \right]$$

In this expression, N is the number of magnetic sites, \vec{S}_i is the atomic spin at site i . The first term corresponds to the exchange energy between spins \vec{S}_i and \vec{S}_j , J_{ij} represents the coupling constant while index j is related to the first nearest magnetic neighbors (V) of atom i . The second term is the Zeeman energy, C_H is a conversion factor allowing the energy to be expressed in Kelvin, while $\|\vec{B}_{\text{ext}}\|$ is in Tesla, and $\|\vec{S}_i\|$ in Bohr magneton (μ_B). The last term corresponds to the uniaxial anisotropy energy with K_{Ui} the uniaxial effective anisotropy constant and \vec{U}_i is a unit vector along the easy magnetization axis. We performed our simulation using Metropolis Monte Carlo algorithm. Temperature T and exchange coupling constant J_{ij} are expressed in Kelvin, the magnetic moments are in μ_B and the anisotropic constant K_{Ui} is in K/atom . At this stage of the work, the surface anisotropy effect is not taken into account. We assume that dipole-dipole interactions are negligible inside core/shell nanoparticle. The role of this interaction becomes more relevant in the case of an assembly of nanoparticles.

The simulation of our core/shell NP requires the knowledge of different magnetic parameters such as

Fig. 1 3D illustration of a core/shell Fe₃O₄/CoO nanoparticle



anisotropy constants, easy magnetization axes, and exchange coupling constants. To perform our calculations, we must choose these parameters for the core, the shell and the magnetic interface between them. For practical reasons, we associate to each atom a type and a magnetic moment according to the nature of the phase it belongs.

Concerning the core, magnetite Fe₃O₄ is a soft ferromagnetic material below 858 K. It crystallizes in an inverse spinel structure. It has a weak bulk anisotropy constant $K_v = -1.35 \times 10^5$ erg/cm³ along [111] direction (Coey 2010). The unit cell consists of 32 oxygen ions (O²⁻) and 24 iron cations distributed in two octahedral (B) and tetrahedral (A) sublattices. The tetrahedral sites are occupied by 8 ${}_A\text{Fe}^{3+}$ cations and the octahedral sites are occupied by 8 ${}_B\text{Fe}^{3+}$ and 8 ${}_B\text{Fe}^{2+}$ cations. Magnetic ions ${}_B\text{Fe}^{3+}$, ${}_B\text{Fe}^{2+}$, and ${}_A\text{Fe}^{3+}$, whose respective types are fixed to 0, 1, and 2, are represented by Heisenberg classical spins while oxygen ions are considered as non-magnetic but allow the superexchange interaction between iron ions. We assume the magnetic moments of iron cations in both sites A and B as $\mu_0 = \mu_1 = 5 \mu_B$ and $\mu_2 = 4 \mu_B$ (Du Trémolet de la Lacheisserie et al. 2000). Concerning the exchange interactions, spins interact via antiferromagnetic superexchange interactions with nearest magnetic neighbors when considering ${}_A\text{Fe}^{3+}-{}_A\text{Fe}^{3+}$ (A–A) or ${}_A\text{Fe}^{3+}-{}_B\text{Fe}^{3+}$ (A–B) bonds, whereas spins interact via ferromagnetic double exchange for ${}_B\text{Fe}^{3+}-{}_B\text{Fe}^{2+}$ (B–B) bonds. The exchange

integrals were taken to be $J_{AA} = -18$ K, $J_{AB} = -28$ K and $J_{BB} = 3$ K in agreement with those reported by Coey in (Coey 2010). Since the core anisotropy is weak, it can be assumed that it is zero or weak in uniaxial direction that simplifies the interpretation of hysteresis loops. We expect the results to be almost independent of this choice.

As far as the shell is concerned, cobalt oxide CoO is an antiferromagnetic material with Néel temperature $T_N = 291$ K. CoO is hard magnetic material with a very high anisotropy value $K_v = 2.7 \times 10^8$ erg/cm³ along the [111] direction (Kanamori 1957). In its face-centered cubic crystallographic structure, each Co^{2+} ion is located in an octahedral position surrounded by 6 O²⁻ ions and vice versa. The Co^{2+} magnetic moment is equal to $\mu_{\text{Co}^{2+}} = 5 \mu_B$ (Du Trémolet de la Lacheisserie et al. 2000). Concerning the exchange interactions, spins interact via antiferromagnetic superexchange interactions with first neighbors (type 3) at an angle of 90° with an exchange integral J_1 and second neighbors (type 4) at an angle of 180° with an exchange integral J_2 . In the literature, we found that ratio J_2/J_1 is -8 in the work of Archer et al. (2008), but 3 in that of Coey (2010). We chose to take the values of $J_1 = -6.9$ K and $J_2 = -21.2$ K as proposed by Coey. It can be noted that those coupling constants lead to frustration.

Concerning the interface, the exchange integrals are not well known in the literature, we therefore assume that the ${}_B\text{Fe}^{3+}$ and ${}_B\text{Fe}^{2+}$ magnetite moments interact

ferromagnetically with Co^{2+} moments; thus, the respective exchange integrals values J_{03} and J_{13} are positive, while $_{\text{A}}\text{Fe}^{3+}$ moments are in an antiferromagnetic coupling with Co^{2+} moments, so the associated exchange integral J_{23} is negative. One can note that type 4 only makes sense within the structure of cobalt oxide to distinguish between first and second neighbors, so no interaction is possible between this type and the spins of the core. Therefore, coupling constants J_{ij} describing the exchange interactions in the nanoparticle can be written as a (5×5) matrix as follows:

$$\begin{pmatrix} J_{ij} \text{ (K)} & \text{BFe}^{3+} & \text{BFe}^{2+} & \text{AFe}^{3+} & \text{Co}^{2+} & \text{Co}^{2+} \\ \text{BFe}^{3+} & 3 & 3 & -28 & J_{03} & 0 \\ \text{BFe}^{2+} & 3 & 3 & 0 & J_{13} & 0 \\ \text{AFe}^{3+} & -28 & 0 & -18 & J_{23} & 0 \\ \text{Co}^{2+} & J_{03} & J_{13} & J_{23} & -6.9 & -21.2 \\ \text{Co}^{2+} & 0 & 0 & 0 & -21.2 & 0 \end{pmatrix}$$

At the interface, the coupling may be zero, weak, intermediate or strong. We focused our work on the choice of different interface coupling constants capable of reproducing the exchange bias coupling properties present in core/shell NPs.

Simulating hysteresis loops by MC

It should be noted that in the frame of classical MC method, one can perform calculations by using a single spin rotation algorithm that works by generating trial moves randomly oriented throughout space. This method is ineffective since the acceptance ratio drops to nearly zero as the temperature approaches zero Kelvin. The efficiency of the simulation can be improved by limiting the new spin orientation in a narrow cone around the direction of the initial spin (Chubykalo et al. 2003; Nehme et al. 2015). This algorithm is called the cone algorithm (CA). Despite this improvement, a crucial problem remains because we are sampling an energy barrier that is not the expected one. Indeed, the acceptance or rejection of a new state/move is based on the Boltzmann probability densities $e^{-\frac{\Delta E}{k_B T}}$ where ΔE is the energy difference between the initial and final states.

The magnetic energy of this system results in the sum of different contributions attributed to exchange interactions (E_{exch}), effective anisotropy (E_{EA}), Zeeman energy (E_{Zeeman}). So, one expresses ΔE as follows: $\Delta E = \Delta E_{\text{exch}} + \Delta E_{\text{EA}} + \Delta E_{\text{Zeeman}}$. Thus, the Boltzmann probability can be written as follows:

$$e^{-\frac{\Delta E}{k_B T}} = e^{-\frac{\Delta E_{\text{exch}}}{k_B T}} \times e^{-\frac{\Delta E_{\text{EA}}}{k_B T}} \times e^{-\frac{\Delta E_{\text{Zeeman}}}{k_B T}}$$

If a simulation is performed falls in the case of the Stoner-Wohlfarth (SW) model (i.e., uniform rotation of magnetization), the corresponding ΔE_{exch} will be zero. As we perform single spin rotations, the rotation of the moments induces an extra/additional energy barrier ($\Delta E_{\text{exch}} \neq 0$), which yields to an extra value of the coercive field H_{c0} called as ‘‘algorithmic contribution’’ because it is provided by the dynamics of the algorithm. The coercive field calculated in the absence of anisotropy corresponds to H_{c0} . Its value is strongly dependent on the field scan speed (FSS), the coupling exchange constant J (i.e., $\Delta E_{\text{exch}} \propto J$) and the dynamics of the algorithm used (CA here). To overcome the induced barrier, one needs to increase NMCS (i.e., work with a slow FSS). This term vanishes to zero when NMCS tends to infinite values (Nehme et al. 2015). The value of the coercive field is then considered as a sum of an algorithmic contribution field (H_{c0}) and a contribution of the effective anisotropy field (H_{EA}) which is directly proportional to the effective anisotropy constant within the validity limit of the SW model. We can thus express the coercive field H_c as follows: $H_c = H_{c0} + H_{\text{EA}}$. On the other hand, the value of the coercive field is given by $H_c = \frac{H_c^+ - H_c^-}{2}$ where H_c^+ and H_c^- stand for positive and negative reversal fields, respectively. Therefore, one can write: $H_c^- = -H_{c0} + H_{\text{EA}}^-$ and $H_c^+ = H_{c0} + H_{\text{EA}}^+$. It follows the following:

- The algorithmic contribution H_{c0} affects equally the negative and positive reversal fields ($H_{c0}^+ = H_{c0}^- = H_{c0}$),
- The negative and positive effective anisotropic fields (H_{EA}^+ and H_{EA}^-), are not necessarily the same especially in the case of a system presenting exchange bias properties, the measured coercive field is then $H_c = \frac{H_c^+ - H_c^-}{2} = H_{c0} + \frac{H_{\text{EA}}^+ - H_{\text{EA}}^-}{2}$,
- The value of the loop shift on the field axis expressed by the exchange field (H_{ex}) is $H_{\text{ex}} = \left| \frac{H_c^+ + H_c^-}{2} \right| = \frac{H_{\text{EA}}^+ + H_{\text{EA}}^-}{2}$.

The measured coercive field depends on the algorithm contribution, while the exchange bias field does not, but depends only on the effective anisotropy.

It is then necessary to measure the algorithmic contribution of the coercive field. This coercive field is a function of the interfacial coupling as one can expect from ΔE_{exch} change and the anisotropic contribution. In the current model, the number of interfacial couplings is negligible compared to the total number of couplings. Therefore, the value of H_{c0} measured for a zero interfacial coupling is taken as a reference. In the following, we note H_c^* the measured value extracted from the MC simulation, once the algorithmic contribution is subtracted from the coercive field.

Results and discussion

Simulated annealing

To obtain the configuration of equilibrium spins by MC simulation, we used the simulated annealing process (Kirkpatrick et al. 1983). Our numerical process starts from a random spin configuration at a high temperature of 1600 K. 10^5 Monte Carlo steps per spin for each temperature were considered during calculations. The temperature of the system is slowly cooled according to the law $T_{i+1} = \alpha_T T_i$ where $\alpha_T = 0.98$ is the coefficient of decrease of the temperature. This process is done for 580 temperature steps to reach a final temperature close to 0.01 K. For the different types, the anisotropy is considered uniaxial according to direction [111]. Figure 2 compares a section at $z = 0$ of the final magnetic configurations obtained without interfacial coupling (a) and for weak interfacial coupling (b).

In the absence of interfacial coupling, the magnetic order is perfectly established in the core: the ${}_B\text{Fe}^{3+}$ and ${}_B\text{Fe}^{2+}$ moments are aligned parallel to each other and antiparallel to the ${}_A\text{Fe}^{3+}$ moments, in agreement with the magnetic structure of magnetite. On the contrary, in the presence of interfacial coupling, these moments remain collinear with each other, but are not always oriented along the [111] direction. It should be noted that in all cases, the moments of cobalt are not collinear because the cationic topology and the AF coupling promote magnetic frustrated interactions. This non-collinearity becomes more important in the contact areas between the core and the shell and can be attributed here to the small size of the NP for which the surface effects (lack

of coordination) are important. The resulting spin configuration obtained for each coupling matrix will subsequently be used as an input file for the hysteresis loop measurements. The external magnetic field will be swept in the direction of the simulated annealing end state.

Study of exchange bias coupling

In all the following cases, the value for the simulation temperature was chosen to be $T = 5$ K in order to study the magnetic properties at low temperature. The simulations have been performed with 601 different steps of field between $+10 T \rightarrow -10 T \rightarrow +10 T$. The external magnetic field is applied in the direction of the final state obtained by the simulated annealing procedure. The hysteresis loop is recorded at a constant FSS and averaged over 20 cycles. The cone algorithm (CA) based on a single spin rotation has been used with an optimal cone radius value $R_{\text{cone}} = 0.1$ (Nehme et al. 2015). The term “reduced magnetization” (M^*) refers to the ratio between the average of the magnetization (M_{tot}) of all magnetic moments constituting the core/shell nanoparticle and the saturation magnetization (M_{sat}) of the magnetite core as follows (A):

$$M^* = \frac{M_{\text{tot}}}{M_{\text{sat}}}, \text{ where } M_{\text{tot}} = \sum_i \frac{n_i M_i}{N} \quad (\text{A}).$$

It should be noted that several simulation tests were performed on our core/shell NP by varying the interfacial coupling matrix. We report here the most significant cases that led us to reproduce EB coupling. Therefore, the interfacial coupling may be weak or strong. The test performed in the absence of any interfacial coupling is done in order to compare the effect of interfacial coupling on the EB properties.

In the case of zero interfacial coupling, the core and the shell are perfectly decoupled. The reversal of the magnetic moments is uniform. The hysteresis loop of the reduced scale magnetization, displayed in Fig. 3 (black curve), is symmetrical and almost square. Saturation magnetization M^* which is close to 1, results from magnetite as the Co^{2+} moments are antiferromagnetically coupled. One can note that the value of the measured coercive field (1.94 T) is significantly larger than the expected one. Theoretically, in the case of uniform rotation, we expect a coercive field that is consistent with the SW model according to the following equation:

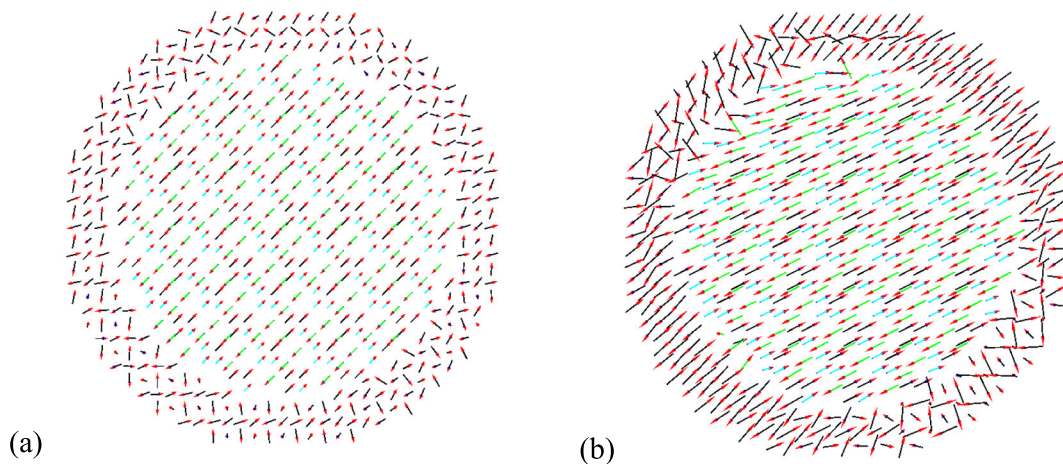


Fig. 2 Representation of a z-section of the final spin configuration obtained in absence (a) and presence (b) of interfacial coupling

$$\begin{aligned} \mu_0 H_c &= \frac{2 K_U}{C_{HM_s}} \\ &= 0.0536 \text{ T} \quad (K_U = 0.024 \text{ K/atom and } M_s = 4/3 \text{ } \mu\text{B}) \end{aligned}$$

The huge difference between the measured and theoretical values is attributed to the algorithmic contribution to the values of the coercive fields by MC (Nehme et al. 2015). Therefore, the value of the extracted field corresponds to the coercive field predicted by SW model ($\mu_0 H_c^* = 0.0536 \text{ T}$).

In the case of weak interfacial coupling, J_{03} and J_{13} were chosen to be 1 K and J_{23} to -1 K . The corresponding hysteresis loop (Fig. 3a) presents a negative shift and an increase in its coercivity in comparison to that obtained for zero interfacial coupling ($\mu_0 H_c^* = 0.23 \text{ T}$). The moments of cobalt are almost blocked under the effect of the field, giving rise to a very low residual magnetization, even negligible. Since our system exhibits a large K_{AF} value, the reversal of AF shell is hard to be completely achieved. The weak interfacial coupling leads to the appearance of a large exchange bias field and partial drag of the interfacial spins of the AF phase; thus, the coercivity is increased. This effect is qualitatively comparable to the observations on the experimental hysteresis loops of the $\text{Fe}_3\text{O}_4/\text{CoO}$ NPs system (Gaudisson et al. 2014; Franceschin et al. 2018).

In the case of strong interfacial coupling, J_{03} , J_{13} , and J_{23} are assumed to be equal to the exchange integrals characteristic of cobalt ferrite CoFe_2O_4 . Indeed, experimental results in this system show that the structure of the sample cannot be described using only two ideal phases (Fe_3O_4 and CoO), but seems much more

complex. Indeed, zero and in-field ^{57}Fe Mössbauer spectrometry measurements reveal the presence of intermediate phase of type $\text{Co}_x\text{Fe}_{1-x}^{2+}\text{Fe}_2^{3+}\text{O}_4$ magnetically hard between the core and the shell resulting from the diffusion of Co^{2+} ions from the shell into the vacancies of the core (Yaacoub et al. 2019). Therefore, we can adopt the coupling matrix of CoFe_2O_4 as an intermediate interfacial coupling matrix. Thus, J_{03} and J_{13} are chosen to be 4 K and J_{23} to -24 K . The corresponding calculated hysteresis loop (Fig. 3b), which is almost symmetrical and larger in width and height, suggests that the magnetization reversal is almost uniform. In fact, the interfacial coupling between the core and the shell is stronger than in the previous case, so the Co^{2+} moments rotate within the external magnetic field. As a result, the coercive field increases ($\mu_0 H_c^* = 0.57 \text{ T}$). Partial polarization of cobalt moments results in significant induced magnetization, increasing the remnant and total saturation magnetization of the system by $0.12 \text{ } \mu\text{B}$.

To highlight the difference between the cases studied, we report in Table 1 the values of interfacial coupling, coercive, and exchange fields, using zero interfacial coupling as reference.

In conventional structures consisting of two simple and different magnetic phases such as bilayers or core/shell nanoparticles, simulation results show (Iglesias et al. 2007b, 2008; Wu et al. 2007) that increasing the value of coupling integrals at the interface improves the exchange field. But this fact is not always in agreement with experimental features. In our detailed model, we show that increasing the strength of interfacial coupling does not necessarily increase the exchange field. It all depends on how the imposed interfacial coupling affects

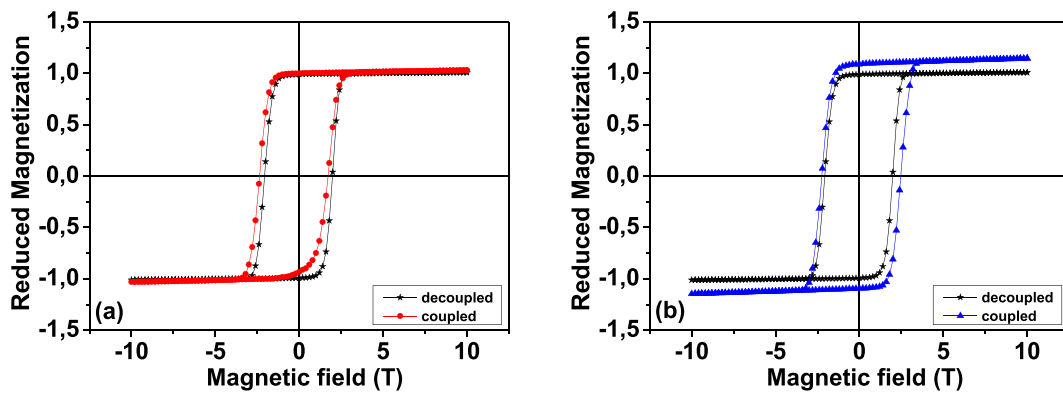


Fig. 3 Hysteresis loops of reduced scale magnetization obtained for weak (a) and strong (b) interfacial coupling in comparison with a zero interfacial coupling (black loops)

interactions between the ions in the cobalt shell and those in the iron core. Here, we have shown that the greatest shift with an increase in coercivity is obtained for the lower interfacial coupling.

Study of inhomogeneous NPs

From an experimental point of view, the structure and the morphology of core-shell NPs could be inhomogeneous formed of core/polycrystalline shell NPs (Gaudisson et al. 2014). It should be noted that there is an epitaxial growth relationship between the core and the shell for different architectures (structural homogeneous or inhomogeneous shell). In order to study the effect of such inhomogeneity on the exchange bias properties, we also modeled the atomic structure of a polycrystalline shell (Fig. 4b). The modeling of this shell uses Voronoi's tessellation with four non-interacting monocrystalline pieces whose size and position are randomly selected. Such a configuration may reduce the magnetic frustration compared to that observed in the case of complete shell, as the interfacial surface is smaller. We consider a distribution of cobalt atoms around the magnetite that mimics the

experimental NPs (Gaudisson et al. 2014; Yaacoub et al. 2019). The resulting NP called core/polycrystalline shell has the same core diameter and shell thickness as the previous NP, which is now called as core/monocrystalline shell NP. Figure 4 summarizes a comparative study between NPs with monocrystalline and polycrystalline shells.

It should be noted that the same study carried out on core/monocrystalline shell NPs for the different values of interfacial coupling was carried out under the same numerical conditions on the core/polycrystalline shell NPs. As an example, we present here the simulated annealing and hysteresis loops obtained in the case of weak interfacial coupling. As schematized in Fig. 4d, the magnetic configuration obtained at 0 K shows that the magnetic moments of the core are collinear and weakly influenced by the coupling in the contact areas with cobalt shell, but the magnetic moments of the shell are disordered near the interface and find their alignment at the outer shell layer.

The corresponding hysteresis loops obtained in the same conditions for the two kinds of NPs are compared in Fig. 4e and f. In the absence of interfacial coupling, the hysteresis loops are obviously symmetrical. For

Table 1 Hysteresis loop characteristics for different coupling strengths

Coupling	J_{03} (K)	J_{13} (K)	J_{23} (K)	$\mu_0 H_c$ (T)	$\mu_0 H_c^*$ (T)	$\mu_0 H_{ex}$ (T)
Zero	0	0	0	1.94	0.053	≈ 0.00
Weak	1	1	-1	2.12	0.23	0.33
Strong	4	4	-24	2.46	0.57	0.04

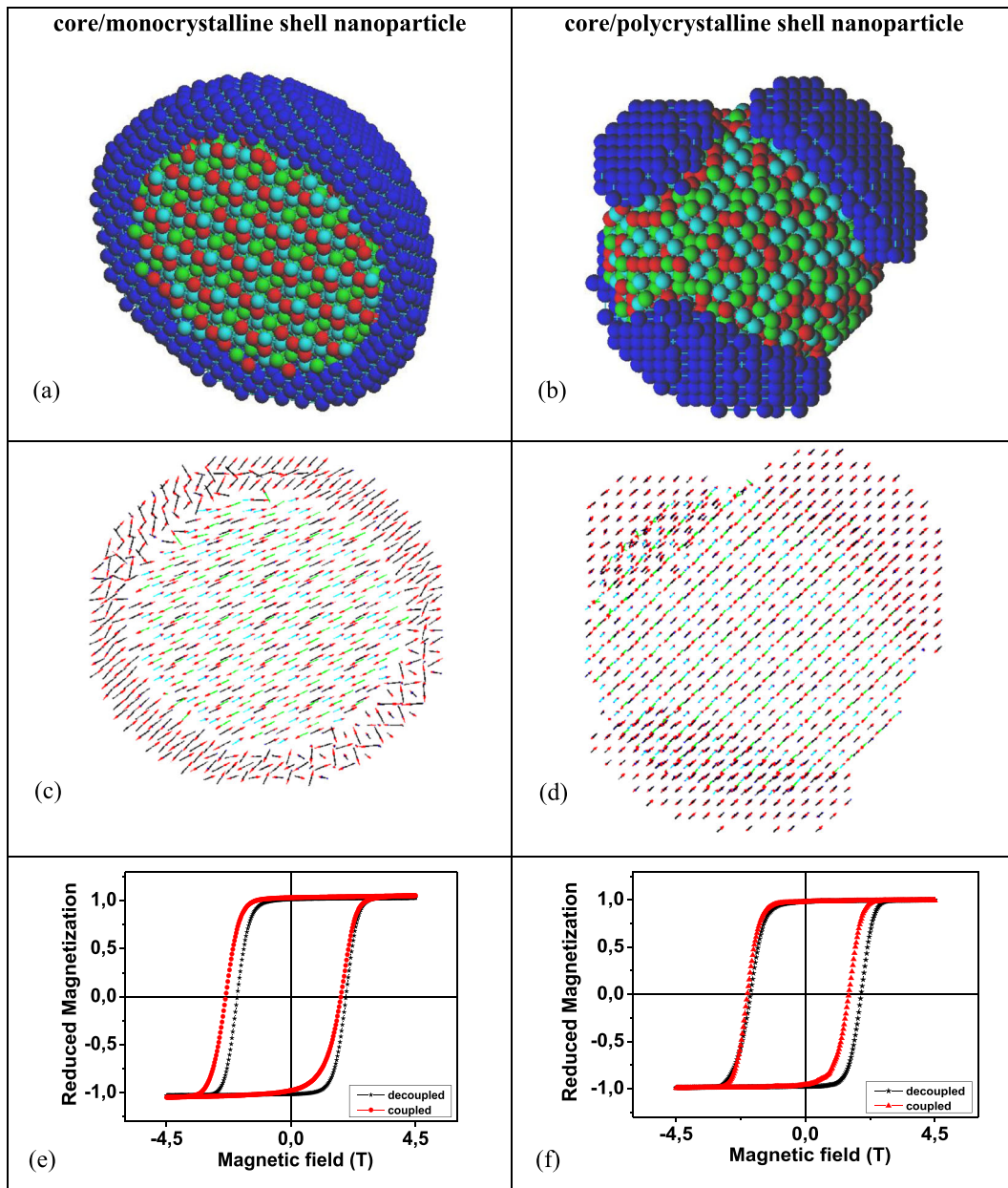


Fig. 4 Numerical modeling of core-shell NP (a, b), magnetic configuration (c, d), and hysteresis cycles (e, f) obtained for core/monocrystalline and core/polycrystalline shell NP, respectively

weak interfacial coupling, the loops of the two NPs present a negative shift, with different shifts of the negative and positive reversal fields (e) and (f). In the case of the core/polycrystalline shell NP, H_c^- remains identical to that of the case of the zero interfacial coupling, but H_c^+ varies, so H_c decreases slightly, whereas it increases slightly in the case of the core/monocrystalline shell NP. This difference can be attributed to the fact that

the configurations presented do not have the same interface density in cobalt ions. It should be noted that we have considered a single nanoparticle, knowing that experimentally the coercive field results from a collective response of thousands of non-homogeneous NPs.

According to Table 2, one can see that the exchange bias field is approximately the same for the two types of core/shell NPs, although the magnetic configurations of

Table 2 Hysteresis loop characteristics for different coupling strengths obtained for core/monocrystalline and core/polycrystalline shell NP

	J_{03} (K)	J_{13} (K)	J_{23} (K)	$\mu_0 H_c$ (T)	$\mu_0 H_c^*$ (T)	$\mu_0 H_{ex}$ (T)
Core/monocrystalline shell	0	0	0	1.96	0.053	≈ 0.00
	1	1	-1	2.08	0.17	0.28
Core/polycrystalline shell	0	0	0	1.94	0.053	≈ 0.00
	1	1	-1	1.76	0.13	0.26

the shell are not the same: the monocrystalline shell is more disordered than the polycrystalline one.

Conclusion

The modeling of nanoparticles at the atomic scale makes it possible to study more precisely the EB phenomenon resulting from the competition between the core and the shell induced by magnetic interfacial interactions. We have shown that increasing the value of coupling integrals at the interface does not systematically improve the exchange field as the literature shows. Indeed, EB coupling depends on the complex matrix of interfacial coupling. However, our numeric model is able to simultaneously reproduce a significant shift in the hysteresis loop and an increase in coercivity for a weak magnetic interfacial coupling in qualitative agreement with the experimental observations on the hysteresis loops of the system under consideration. In addition, the coercive field is reinforced for a stronger interfacial magnetic coupling, i.e., the interfacial coupling constants are assumed to be identical to those of cobalt ferrite. We have also shown that taking into account the morphology of the NPs slightly influences the properties of EB. The tendency of the present results seems fairly consistent with the observations made on the experimental hysteresis loops of core-shell NPs' system (Gaudisson et al. 2014; Franceschin et al. 2018; Flores-Martinez et al. 2018, n.d.).

It should be noted that our built core/shell NP remains an approximate model that tends to mimic the experimental system. To achieve this objective and better establish the morphology-EB relationship and magnetic properties, there is still a lot of work to be done. The model must first be improved by considering an intermediate phase of cobalt ferrite between the core and the shell as experimentally established, resulting in a realistic but more complex core/shell/shell morphology. The main problem here is to manage/control the

presence of two interfaces for which the values of the magnetic coupling constants remain difficult to estimate. In addition, the increasing number of atoms makes the computation time very long. A second approach consists in describing a complete polycrystalline shell as a random tiling of single crystalline pieces: in this case, the problems are related to the increasing contribution of interfacial zones (between pieces and between piece and core). Such modeling approaches are under way.

Compliance with ethical standards

Conflict of interest The authors declare that they have no conflict of interest.

References

- Archer T, Hanafin R, Sanvito S (2008) Magnetism of CoO polymorphs: density functional theory and Monte Carlo simulations. *Phys Rev B* 78:2–6. <https://doi.org/10.1103/PhysRevB.78.014431>
- Bader SD (2006) Colloquium: opportunities in nanomagnetism. *Rev Mod Phys* 78:1–15. <https://doi.org/10.1103/RevModPhys.78.1>
- Balamurugan B, Sellmyer DJ, Hadjipanayis GC, Skomski R (2012) Prospects for nanoparticle-based permanent magnets. *Scr Mater* 67:542–547. <https://doi.org/10.1016/j.scriptamat.2012.03.034>
- Bedanta S, Kleemann W (2009) Supermagnetism. *J Phys D Appl Phys* 42:013001. <https://doi.org/10.1088/0022-3727/42/1/013001>
- Binns C, Domingo N, Testa AM, Fiorani D, Trohidou KN, Vasilakaki M, Blackman JA, Asaduzzaman AM, Baker S, Roy M (2010) Interface exchange coupling in Co nanoparticles dispersed in a Mn matrix. *J Phys Condens Matter* 22:436005. <https://doi.org/10.1088/0953-8984/22/43/436005>
- Chandra S, Khurshid H, Li W, Hadjipanayis GC, Phan MH, Srikanth H (2012) Spin dynamics and criteria for onset of exchange bias in superspin glass Fe/ γ -Fe₂O₃ core-shell nanoparticles. *Phys Rev B* 86:014426. <https://doi.org/10.1103/PhysRevB.86.014426>

- Chubykalo O, Nowak U, Smirnov-Rueda R, Wongsam MA, Chantrell RW, Gonzalez JM (2003) Monte Carlo technique with a quantified time step: application to the motion of magnetic moments. *Phys Rev B* 67. <https://doi.org/10.1103/PhysRevB.67.064422>
- Coe JMD (2010) *Magnetism and magnetic materials*. Cambridge
- De D, Iglesias Ó, Majumdar S, Giri S (2016) Probing core and shell contributions to exchange bias in Co/Co₃O₄ nanoparticles of controlled size. *Phys Rev B* 94:184410. <https://doi.org/10.1103/PhysRevB.94.184410>
- Du Trémolet de la Lacheisserie E, Cyrot M, Decorps M, Dieny B, Geoffroy O, Gignoux D, Lacroix C et al (2000) *Magnétisme I- Fondements*, EDP Sciences. ISBN 10: 2868834639
- Duan C, Wang W, Xie Q (2013) Review article: fabrication of nanofluidic devices. *Biomicrofluidics* 7:026501. <https://doi.org/10.1063/1.4794973>
- Estrader M, López-Ortega A, Estradé S, Golosovsky IV, Salazar-Alvarez G, Vasilakaki M, Trohidou KN, Varela M, Stanley DC, Sinko M, Pechan MJ, Keavney DJ, Peiró F, Suriñach S, Baró MD, Nogués J (2013) Robust antiferromagnetic coupling in hard-soft bi-magnetic core/shell nanoparticles. *Nat Commun* 4:2960. <https://doi.org/10.1038/ncomms3960>
- Flores-Martínez N, Franceschin G, Gaudisson T, Beauvier P, Yaacoub N, Grenèche JM, Valenzuela R, Ammar S (2018) Giant exchange-bias in polyol-made CoFe₂O₄-CoO core-shell like nanoparticles. *Part Part Syst Charact* 35:1–8. <https://doi.org/10.1002/ppsc.201800290>
- Flores-Martínez N, Franceschin G, Gaudisson T, Derouich SG, Haj-Khlifa S, Yaacoub N, Grenèche JM, Menguy N, Valenzuela R, Ammar S (n.d.) On the first evidence of exchange-bias feature in magnetically contrasted consolidates made from CoFe₂O₄-CoO core-shell nanoparticles. *Scientific Reports* (in revision)
- Franceschin G, Gaudisson T, Menguy N, Dodrill Brad C, Yaacoub N, Grenèche JM, Valenzuela R, Ammar S (2018) Exchange-biased Fe_{3-x}O₄-CoO granular composites of different morphologies prepared by seed-mediated growth in polyol: from core-shell to multicore embedded structures. *Part Part Syst Charact* 35:1800104. <https://doi.org/10.1002/ppsc.201800104>
- Gaudisson T, Ourry L, Hammoud H, Nowak S, Menguy N, Yaacoub N, Grenèche JM, Mammari F, Ammar S (2014) Exchange-biased oxide-based core-shell nanoparticles produced by seed-mediated growth in polyol. *J Nanopart Res* 16:2359. <https://doi.org/10.1007/s11051-014-2359-5>
- Gleiter H (1989) Nanocrystalline materials. *Prog Mater Sci* 33: 223–315. [https://doi.org/10.1016/0079-6425\(89\)90001-7](https://doi.org/10.1016/0079-6425(89)90001-7)
- Iglesias Ó, Batlle X, Labarta A (2007a) Modelling exchange bias in core/shell nanoparticles. *J Phys Condens Matter* 19: 406232. <https://doi.org/10.1088/0953-8984/19/40/406232>
- Iglesias Ó, Batlle X, Labarta A (2007b) Exchange bias and asymmetric hysteresis loops from a microscopic model of core/shell nanoparticles. *J Magn Magn Mater* 316:140–142. <https://doi.org/10.1016/j.jmmm.2007.02.057>
- Iglesias Ó, Labarta A, Batlle X (2008) Phenomenology and models of core/shell nanoparticles. *J Nanosci Nanotechnol* 8:2761–2780. <https://doi.org/10.1166/jnn.2008.015>
- Jun YW, Lee JH, Cheon J (2008) Chemical design of nanoparticle probes for high-performance magnetic resonance imaging. *Angew Chem Int Ed* 47:5122–5135. <https://doi.org/10.1002/anie.200701674>
- Kanamori J (1957) Theory of the magnetic properties of ferrous and cobaltous oxides, II. *Prog Theor Phys* 17:197–222. <https://doi.org/10.1143/PTP.17.197>
- Kechrakos D, Trohidou KN (1998) Magnetic properties of dipolar interacting single-domain particles. *Phys Rev B* 58:1216–12177. <https://doi.org/10.1103/PhysRevB.58.12169>
- Kirkpatrick S, Gelatt CD, Vecchi MP (1983) Optimization by simulated annealing. *Science* 220:671–680. <https://doi.org/10.1126/science.220.4598.671>
- Manna PK, Yusuf SM (2014) Two interface effects: exchange bias and magnetic proximity. *Phys Rep* 535:61–99. <https://doi.org/10.1016/j.physrep.2013.10.002>
- Margaris G, Trohidou KN, Nogués J (2012) Mesoscopic model for the simulation of large arrays of bi-magnetic core/shell nanoparticles. *Adv Mater* 24:4331–4336. <https://doi.org/10.1002/adma.201200615>
- Nehme Z, Labaye Y, Sayed Hassan R, Yaacoub N, Grenèche JM (2015) Modeling of hysteresis loops by Monte Carlo simulation. *AIP Adv* 5:0–11. <https://doi.org/10.1063/1.4938549>
- Nogués J, Sort J, Langlais V, Skumryeva V, Suriñach S, Muñozb JS, Baró MD (2005) Exchange bias in nanostructures. *Phys Rep* 422:65–117. <https://doi.org/10.1016/j.physrep.2005.08.004>
- O'Grady K, Fernandez-Outon LE, Vallejo-Fernandez G (2010) A new paradigm for exchange bias in polycrystalline thin films. *J Magn Magn Mater* 322:883–899. <https://doi.org/10.1016/j.jmmm.2009.12.011>
- Ong QK, Xin ML, Wei A (2012) Role of frozen spins in the exchange anisotropy of core-shell Fe@Fe₃O₄ nanoparticles. *J Phys Chem C* 115:2665–2672. <https://doi.org/10.1021/jp110716g>
- Skumryev V, Stoyanov S, Zhang Y, Hadjipanayis G, Givord D, Nogués J (2003) Beating the superparamagnetic limit with exchange bias. *Nature* 423:850–853. <https://doi.org/10.1038/nature01750.1>
- Tartaj P, Morales MDP, Veintemillas-Verdaguer S, González-Carreño T, Serna CJ (2003) The preparation of magnetic nanoparticles for applications in biomedicine. *J Phys D Appl Phys* 36:R182–R197. stacks.iop.org/JPhysD/36/R182
- Terris BD, Thomson T (2005) Nanofabricated and self-assembled magnetic structures as data storage media. *J Phys D Appl Phys* 38(38):R199–R222. <https://doi.org/10.1088/0022-3727/38/12/R01>
- Thorat ND, Khot VM, Salunkhe AB, Prasad AI, Ningthoujam RS, Pawar SH (2013) Surface functionalized LSMO nanoparticles with improved colloidal stability for hyperthermia applications. *J Phys D Appl Phys* 46:105003. <https://doi.org/10.1088/0022-3727/46/10/105003>
- Vasilakaki M, Trohidou KN, Nogués J (2015) Enhanced magnetic properties in antiferromagnetic-core/ferrimagnetic-shell nanoparticles. *Sci Rep* 5:9609. <https://doi.org/10.1038/srep09609>
- Wu MH, Li QC, Liu JM (2007) Monte Carlo simulation of size, random field and temperature dependences of exchange bias in a core/shell magnetic nanoparticle. *J Phys Condens Matter*

- 19:186202. <https://doi.org/10.1088/0953-8984/19/18/186202>
- Yaacoub N, Mortada H, Nehme Z, Grenèche J (2019) Chemical inhomogeneity in iron oxide @ CoO core-shell nanoparticles : a local probe study using zero-field and in-field ^{57}Fe Mössbauer spectrometry. *J Nanosci Nanotechnol* 19:5014–5019. <https://doi.org/10.1166/jnn.2019.16794>
- Zaim A, Kerouad M (2010) Monte Carlo simulation of the compensation and critical behaviors of a ferrimagnetic core/shell nanoparticle Ising model. *Phys A Stat Mech Appl* 389:3435–3442. <https://doi.org/10.1016/j.physa.2010.04.034>
- Zaim A, Kerouad M, EL Amraoui Y (2009) Magnetic properties of a ferrimagnetic core/shell nanocube Ising model: a Monte Carlo simulation study. *J Magn Magn Mater* 321:1077–1083. <https://doi.org/10.1016/j.jmmm.2008.10.009>
- Zianni X, Trohidou K (1999) Magnetization reversal mechanisms in small antiferromagnetic particles. *J Appl Phys* 85:1050–1057. <https://doi.org/10.1063/1.369227>

Publisher's note Springer Nature remains neutral with regard to jurisdictional claims in published maps and institutional affiliations.